Colloids and Surfaces B: Biointerfaces 161 (2018) 27–34

Contents lists available at ScienceDirect

Colloids and Surfaces B: Biointerfaces

journal homepage: www.elsevier.com/locate/colsurfb

Full Length Article

Synergy in thrombin-graphene sponge for improved hemostatic efficacy and facile utilization

Guofeng Li[a], Kecheng Quan[a], CongCong Xu[a], Bo Deng[b], Xing Wang[a,*]

[a] The State Key Laboratory of Chemical Resource Engineering, Beijing Laboratory of Biomedical Materials, Beijing University of Chemical Technology, Beijing, 100029, PR China

[b] Department of Oncology of Integrative Chinese and Western Medicine, China-Japan Friendship Hospital, Beijing, 100029, PR China

ARTICLE INFO

Article history:
Received 23 July 2017
Received in revised form 4 October 2017
Accepted 6 October 2017
Available online 10 October 2017

Keywords:
Graphene
Thrombin
Composite
Hemostasis
Synergy effect

ABSTRACT

Composites are attractive for its potential synergistic effects that can result in high-performance, but the synergy depends on subtle design. In this study, a hemostatic composite, a thrombin/cross-linked graphene sponge (TCGS), was developed through a facile gradient composite strategy. The porous structure of the CGS assures that the thrombin is stably embedded in the TCGS, avoiding a burst release but maintaining its bioactivity. In the synergy between proper thrombin stimulation and the fast absorption of the sponge, TCGS exhibits outstanding hemostatic performance, ultrafast bleeding cessation, within 100 s, which is superior to both CGS and equal amounts of native thrombin. Lower or excessive thrombin dosages prolong the bleeding time. The study revealed that the balance between plasma absorption and thrombin stimulation at the interface is critical for improving hemostatic efficacy. TCGS is also highlighted for its biosafety and stability, even after 6 months of storage in environment. This potentially ultra-long shelf life is conducive to its practical applications. Therefore, TCGS not only provides a new strategy for developing a hemostatic composite but also provides a new method and understanding for the design of hemostatic materials.

1. Introduction

The use of hemostatic agents is critical for saving lives from rapid blood loss from a variety of causes, such as surgical treatments or traumatic accidents, because massive hemorrhage leads to a great threat of death [1–4]. Currently, the commonly used hemostatic agents are generally classified as either inorganic clay (such as zeolite, mesoporous silica and kaolinite) [5], or organic materials (such as chitosan, gelatin and fibrin) [6,7] and their composites [8–10]. Compared with the former two kinds of hemostats, composites of these materials have advantages for improvement of hemostatic performance, while minimizing their shortcomings [11]. For example, silicate-gelatin hydrogel inherits the separate, excellent properties of injectability, rapid mechanical recovery, physiological stability, and an ability to promote coagulation [12]. Chitosan wound dressing is refined by incorporating polyphosphate to increase platelet adhesion and plasma absorption that accelerates blood clotting [13]. Therefore, suitable hemostatic composites are advantageous in their hemostatic performance and biosafety.

Cross-linked graphene sponge (CGS) is a new hemostat with great potential for treatment of trauma [14]. It rapidly absorbs plasma, accelerating coagulation. But, the shortcoming of CGS is that, when in contact with blood, it cannot stimulate hemocytes to promote bleeding control. To enhance the hemostatic ability of CGS, increasing the charge density [15] and incorporating clay [16] have been attempted to enhance its performance effectively. Further, those studies demonstrated that CGS can work as an alternative platform to carry different hemostatic mechanisms. Thus, creating a novel composite with a new active mechanism is important to achieve a high-performance of hemostasis.

Thrombin, a serine proteinase known as the activated coagulation factor II, is widely used for hemostasis [17–19]. It can directly convert fibrinogen into fibrin, polymerizing strong fibrin clots in the coagulation cascade [20,21]. However, thrombin may also cause hypersensitivity reactions, and severe bleeding and transmit infections or thrombosis, when improperly used [22–25]. To meet the demands of security and stability, thrombin-based composites were developed, such as the loading of thrombin into a polymeric microsphere [26–28], or immobilizing it in a gelatin matrix [29–32]. However, those composites mainly target in-body

* Corresponding author.
E-mail address: wangxing@mail.buct.edu.cn (X. Wang).

https://doi.org/10.1016/j.colsurfb.2017.10.021
0927-7765/

hemostasis. Although the side effects of thrombin are reduced for this composite, there still exists the risk of a high internal dosage of thrombin that would be completely absorbed by the patient [33–35]. Therefore, utilizing thrombin's function while avoiding the risks of excess release and dwelling should be highlighted. Based on the aforementioned CGS used as a suitable supporter, the combination of thrombin as a bio-safe and effective trauma hemostat is thus desired and valuable.

In this study, we developed a facile spray method to prepare thrombin-coated CGS (TCGS) composites. Thrombin is absorbed into the CGS in a gradient manner due to the porous sponge structure. The inside surfaces of CGSs are known as reduced graphene oxide [14], which is effective in immobilizing thrombin-like protein [36]. This property helps the TCGS to prevent a burst release of thrombin and maintain its bioactivity within the small cavities of the sponge structure. Therefore, a suitable amount of thrombin on TCGS not only ensures the fast absorbability by the fundamental CGS supporter but also triggers the coagulation pathway as soon as thrombin comes in contact with blood. In a potential synergistic effect of the above-mentioned two mechanisms, this TCGS composite is expected to be a new thrombin based trauma hemostat.

2. Experimental

2.1. Materials

Thrombin was obtained from Peking University Third Hospital. Coomassie Brilliant Blue G-250 (CBB) was purchased from Tokyo Chemical Industry (TCI). Chloral hydrate was purchased from Sigma. Sprague-Dawley (SD) rats were purchased from Vital (Charles) River Laboratory, Beijing, China. Fresh blood was obtained from the SD rat, and the anticoagulant (ACD) whole blood was prepared by combining fresh blood and citrate dextrose in the ratio of 9:1 [37]. Other commonly used chemical reagents were purchased commercially. All of the SD rats used for animal experiment in this research were treated and cared for in accordance with the National Research Council's Guide.

2.2. Preparation of TCGS

First, CGS was prepared according to the procedures in the literature procedures [14]. Briefly, 200 μL of ethylenediamine (EDA) was mixed with 20 mL of graphene oxide (GO) dispersion (3 mg mL^{-1}). The mixture was heated to 96 °C for 6 h in a reaction kettle to obtain a GO hydrogel. After freeze-drying and Soxhlet extraction by alcohol, the purified GO aerogel was dried and treated with microwave radiation (800 W, 5 s) to obtain the CGS. Then, thrombin solution (1 mL, 25 U mL^{-1}, where U is unit of activity) was sprayed uniformly onto the surface of the CGS. The composite material was kept at room temperature for 5 min and then underwent freeze-drying for 24 h to immobilize the thrombin, forming the named TCGS.

2.3. Thrombin distribution

Fluorescence image analysis. Water-soluble fluorescent labels (strontium aluminate and polyacrylic acid suspension, purchased from Shanghai Future Industrial Co., Ltd.) were diluted with water (1/4, v/v) and dissolved with thrombin. The mixed thrombin solution (1 mL, 25 U mL^{-1}) was sprayed on the surface of the CGS. The final material was obtained after freeze-drying. After UV (365 nm) irradiation for 5 min, fluorescent of the labelled TCGS could be observed in a darkroom.

Quantitative analysis. TCGS was equally divided into three layers: the top layer, the middle layer and the bottom layer (as shown in Fig. 1c inset). Each layer was stirred at a high velocity for 1 h in 20 mL of deionized water to elute the immobilized thrombin. One mL eluent was mixed with 4 mL CBB standard liquid. The mixture was measured by an ultraviolet spectrophotometer (MAPADA UV-1100) at 595 nm. The thrombin content of each layer was calculated by the thrombin-CBB standard curve [38].

2.4. Stability of the modified thrombin in TCGS

The TCGS was immersed in 20 mL of deionized water and extracted or slowly stirred (300 rpm) for 5 min. Then, 1 mL of the obtained extract was mixed with 4 mL of CBB standard liquid. The mixture was measured by a spectrophotometer (MAPADA UV-1100) at 595 nm. The untreated deionized water was served as a negative control, and the equivalent concentration of thrombin (2.5 U mL^{-1}) served as a positive control. The thrombin content of each group was calculated using the thrombin-CBB standard curve [38].

2.5. Blood cell evaluations

Morphology Study of Blood Cells. The ACD-whole blood was directly applied onto the top layer of the TCGS. After 3 min, a layer of blood scab was formed, and excess phosphate buffer solution (PBS) was added 3 times to rinse the free blood cells. Then, the material was immobilized with 2.5% glutaraldehyde for 2 h. To dehydrate, the immobilized blood cells were immersed in a graded ethanol series (50%, 60%, 70%, 80%, 90% and 100%) for 10 min. The sample was freeze-dried and metal-sprayed in preparation for scanning electron microscopy (SEM, S-4700 Hitachi) observation [39].

Blood Cell Select Adhesion. The top layer of the TCGS was equilibrated in 20 mL of PBS for 2 h at 37 °C. Then 1 mL of ACD-whole blood was added and allowed to fully contact for 1 h at 37 °C. PBS was added 3 times to remove the blood cells that did not adhere on the TCGSs. Then, the material was immobilized with 2.5% glutaraldehyde for 2 h. To dehydrate, the immobilized blood cells were immersed in a graded ethanol series (50%, 60%, 70%, 80%, 90% and 100%) for 10 min. The sample was freeze-dried and metal-sprayed before SEM observation.

Platelet Adhesion. For the platelet selective adhesion test, the top layer of the TCGS was equilibrated in 20 mL of PBS for 2 h at 37 °C. Then, 2 mL of platelet-rich plasma (PRP), which was separated from the ACD-whole blood by centrifuge at 2000 × g for 20 min at 4 °C, was added to allow fully contact for 1 h at 37 °C. PBS was added 3 times to remove the blood cells that did not adhere to the TCGS. Then, the material was immobilized with 2.5% glutaraldehyde for 2 h. To dehydrate, the immobilized blood cells were immersed in a graded ethanol series (50%, 60%, 70%, 80%, 90% and 100%) for 10 min. The sample was freeze-dried and metal-sprayed before SEM observation [40,41].

2.6. In vitro clotting tests

Approximately 50 μL of fresh blood was added into test samples to react for 30, 60, 120, 180 and 240 s. The tested samples included the CGS, the TCGS and native thrombin. The CGS and TCGS were prepared into equal volumes. The amount of native thrombin was equal to that in the TCGS, and the native thrombin was dissolved in 10 μL of deionized water. Blood without a reaction was served as a blank control. After each reaction time, 10 mL of deionized water was added to dissolve free red blood cells, with a slightly shaking. Then, the solutions were measured by UV at 542 nm and the content of the hemoglobin for each sample at each time point was calculated by the following equation: Hemoglobin absorbance = $Is/Ir \times 100\%$, where Is is the absorbance of the resulting sample, and Ir is the absorbance of the blank control [42,43].

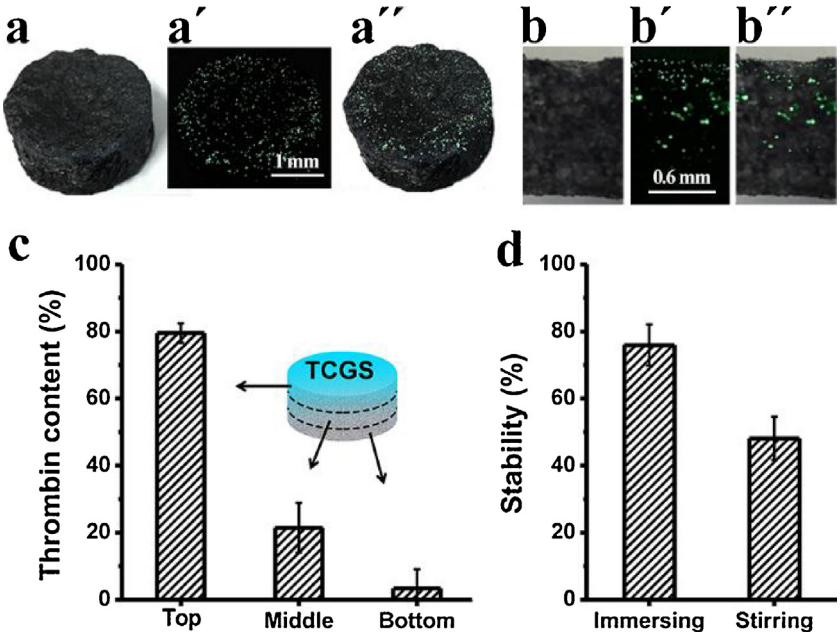

The distribution of the fluorescence-labelled thrombin (a–aíí) on the surface and (b–bíí) in the inner region of the TCGS. (a) and (b) are bright field images. (aí) and (bí) are fluorescence images. (aíí) and (bíí) are merged images. (c) Quantitative analysis of the thrombin in TCGS. (d) Stability of the modified thrombin in TCGS. Data values correspond to mean ± SD (n = 3).

2.7. Rat tail amputation test

Male SD rats, approximately 7 weeks old, were raised for 3 days in a standard environment prior to the operation. The rats were anesthetized with 10% chloral hydrate (w/v) at the ratio of 0.5 mL per 100 g. The rat tail was cut at a point half of the total length (at approximate 7 cm). Then, the sponge material was pressed on the wound section and the bleeding time was recorded. In the gradient thrombin hemostasis evaluation, 25 U, 50 U, 100 U 150 U and 200 U of thrombin were dissolved in 1 mL of deionized water in centrifuge tubes separately, and the wound section of the rat tails was immersed in the tubes for bleeding control.

3. Results and discussions

3.1. Material characterization

Typically, the TCGS was prepared by immobilizing 25 U of thrombin onto its surface through a spray method. Water-soluble fluorescent labels (strontium aluminate) were mixed and sprayed together with thrombin to investigate their distribution within the TCGS. By visible observation, it is clear that the fluorescence is evenly distributed on the surface of the TCGS, whereas its intensity progressively decreases within the interior (Fig. 1a and b). This fact shows that thrombin is mainly retained on the top layer of the TCGS. When the CBB standard liquid was used to quantify the immobilized thrombin, the result was consistent, in that approximately 80% of thrombin dispersed onto the top layer of the TCGS, while the remainder gathered mostly in the middle layer (Fig. 1c). This distribution way of thrombin favors of hemostatic performance because the immobilized thrombin on the surface of the TCGS can directly contact the wound and rapidly trigger the coagulation pathway to stop the bleeding.

The physical stability of the immobilized thrombin in the TCGS was evaluated. As shown in Fig. 1d, after 5 min immersion, approximately 80% of thrombin remained in the TCGS. Even after stirring, the remaining thrombin was up to 50%, indicating that thrombin strongly adhered to the graphene layers because of the porous structure of the TCGS. Moreover, during the actual hemostatic process, the contacting time (<2 min) between the thrombin and the blood vessels was far shorter than the reaction time (5 min). The thrombin on the surface of the graphene layer was difficult to remove from the TCGS or to diffuse into blood vessels, which ensured the biosafety of the TCGS.

3.2. Interaction with blood cell

Thrombin is a promoting factor in the coagulation cascade [44,45]. Absorption of it within the CGS is aimed at enhancing the interfacial stimulation ability of the composite TCGS. Thus, morphology studies of hemocytes and platelets on the sponge surface were carried out to evaluate the bioactivity of the adhered thrombin.

First, a drop of blood was dropped onto the surface of the TCGS. The plasma was absorbed quickly due to its porous structure, leaving a layer of hemocytes on the surface of the TCGS (Fig. 2a). We know that gathering of hemocytes onto the CGS will stimulate their normal physiological status and accelerate the coagulation process to form clotting [14,15]. Therefore, we see a cellular cake on the surface. However, for this TCGS, in addition to promoting the gathering of hemocytes, it also caused large amounts of filamentous mesh to develop, which trapped the platelets and hemocytes to form a quilt, as shown in Fig. 2aí. Direct evidence shows that thrombin in the composite remarkably affects blood clotting at the interface, since thrombin can activate soluble fibrinogen into insoluble fibrin, thus forming a strong thrombus. On the basis of the formation of the filamentous mesh, we deduced that the thrombin immobilized in the TCGS maintained its bioactivity and was able to perform its biocatalytic function during the clotting process.

Next, selective adhesion tests were performed to determine whether the surface of the TCGS could stimulate hemocytes [20,21]. As shown in Fig. 2b,bí, although there were a large number of erythrocytes adhering to the surface, the material surface did not affect their physiological status, as they all maintained a normal shape. This phenomenon indicates that TCGS is biocompatible with erythrocytes. However, TCGS could effectively activate platelets, as shown in Fig. 2c,cí. The platelets stretched out pseudopodia and changed their shape on the surface of TCGS. An active platelet can

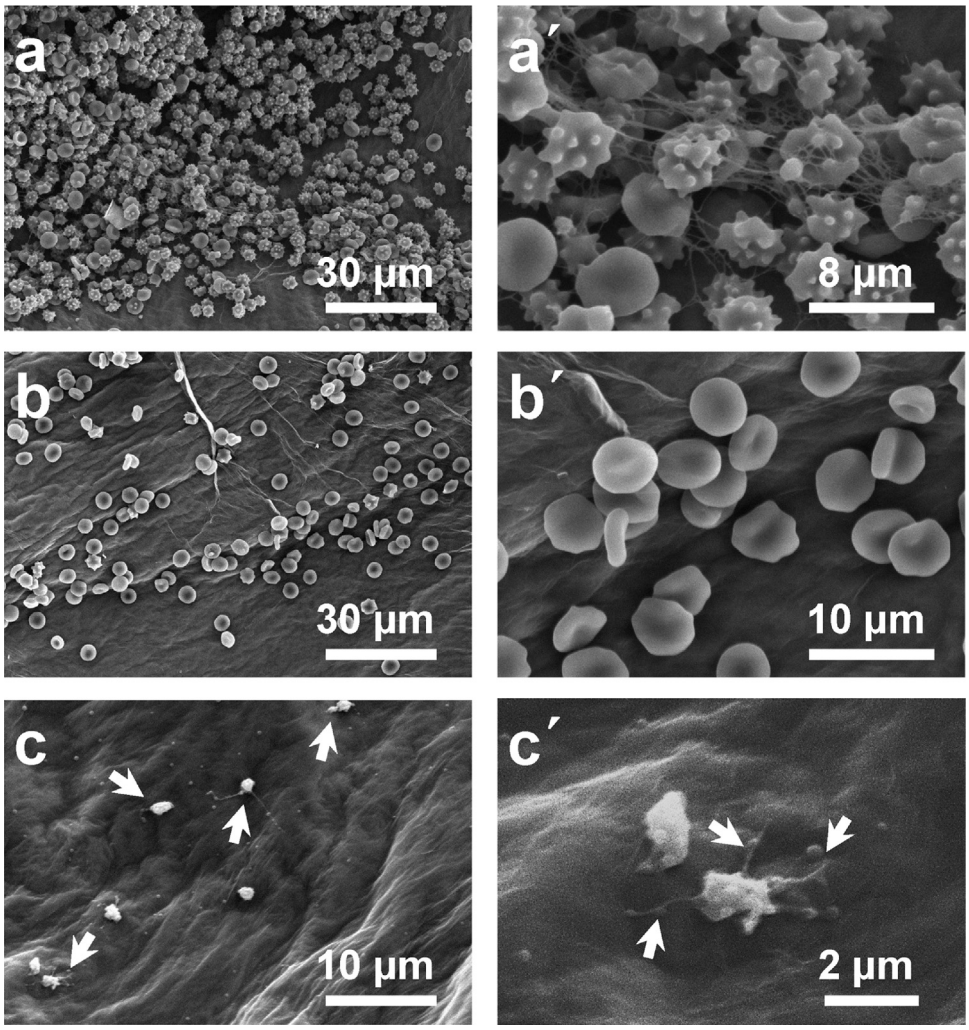

SEM images of blood cells and platelet adhesion on the TCGS surface. (a) Morphology of whole blood fast absorption. (aí) Fibrin formed and trapped hemocytes. Selective adhesion of (b) blood cells and (c) platelets. (bí) Blood cells with a regular shape. (cí) Platelets with stretched out pseudopodia. The arrows showed the active platelets.

support a burst of thrombin generation on its surface. The produced thrombin can sequentially trigger fibrinogen, converting to a stable fibrin clot [46,47]. In this case, it is mainly due to the thrombin's stimulation rather than the effect of the CGS [48].

3.3. In vitro blood clotting

Blood clotting tests in vitro were initially adopted to evaluate the hemostatic performance of the TCGS. As control groups, equivalent thrombin and untreated CGSs were also investigated using the same approach. Fig. 3a exhibits a schematic diagram of the clotting test. Fresh blood was directly dropped onto the samples. After different periods of interaction, deionized water was added to dissolve the free hemoglobin, which was released from the unclotted erythrocytes. Fig. 3b shows the statistical analysis. At the first 30 s, more than 70% of erythrocytes were coagulated in the TCGS and native thrombin groups, while only 45% of erythrocytes were clotted in the CGS group. After a prolonged time of action, blood gradually coagulated and formed a solid clot. The hemoglobin concentration decreased to less than 20% after 60 s. Therefore, the TCGS displayed better clotting results than thrombin. These results indicated that TCGS accelerates blood coagulation.

However, the clotting capabilities of TCGS approximated those of simple CGS. To reveal its advantage, ACD-whole blood was used to repeat the above test. ACD-whole blood is harder to coagulate because of the absence of anticoagulants [49]. In this way, the clotting rate can be slowed, and the differences in clotting capabilities can be magnified. As shown in Fig. 3c, the CGS promotes only 20% ACD-whole blood clotting within 60 s. However, more than 88% of the ACD-whole blood in the TCGS clotted within the same period, while the data in the native thrombin is 80%. In addition, the solution extracted from the TCGS (the middle tube of Fig. 3c inset) is distinctly lighter than that from the native thrombin (the right tube of Fig. 3c inset). The result shows that the TCGS is more efficient than native thrombin for accelerating blood clotting.

3.4. In vivo hemostatic efficacy

The rat-tail amputation model was served as an in vivo evaluation. As shown in Fig. 4, the mean hemostasis time of the TCGS was 100.0 ± 15.5 s, which is 101.0 s shorter than that of the CGS (201.0 ± 46.0 s). Meanwhile, an equivalent thrombin coating on gauze (TG) was also tested as a control group. Its hemostatic time, however, is prolonged to 250.0 ± 75.5 s. Although faster than the naked gauze (more than 10 min) [14], TG is significantly slower than the TCGS in stopping bleeding ($p < 0.01$). Therefore, this fact shows that the modified thrombin in the TCGS has dramatically improved the hemostatic efficiency of the CGS. The ultrafast hemostatic performance of the TCGS is based on two mechanisms: fast absorption and thrombin stimulation. Only thrombin stimulation

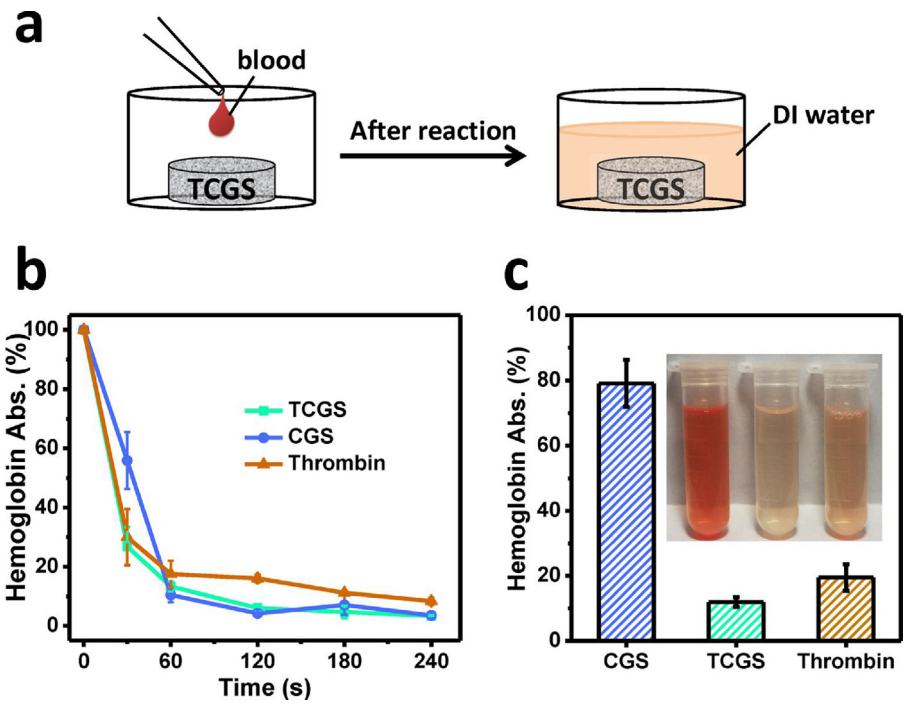

Clotting test results for different reaction conditions. (a) Schematic illustration of the in vitro clotting test. (b) The TCGS and controls reacted with fresh blood for 30, 60, 120, 180 and 240 s respectively. (c) The TCGS and controls reacted with ACD-whole blood for 60 s. The inset shows the corresponding aqueous solutions of hemoglobin after the reaction. Data values correspond to the mean ± SD (n = 3).

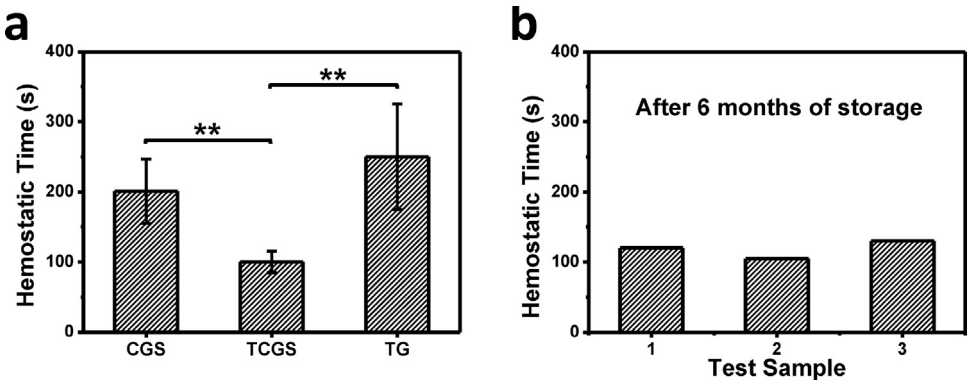

(a) The hemostatic time of the TCGS and controls in the rat-tail amputation model. Data values corresponded to the mean ± SD, n = 6. Two-way ANOVA, ** $p < 0.01$, representing a significant difference compared with the controls. (b) The hemostatic time of the TCGS after storing for 6 months at room temperature condition (n = 3).

does not dominate the hemostatic activity, according to the hemostatic efficiency of TG.

Since thrombin related products are usually stored at low temperature (below 10 °C), biological activity of the immobilized thrombin in TCGS was thus evaluated. We stored the TCGSs at room temperature (25 ± 5 °C) for over 6 months. Those TCGSs could still perform ultrafast hemostasis, with a recorded hemostatic time of 118.3 ± 12.6 s (Fig. 4b, n = 3). These values are very similar to those of the fresh TCGS. Thus, it can be act as a durable and convenient hemostatic agent.

3.5. *Influence of thrombin amount*

Different additional amounts of thrombin were investigated. First, the thrombin solutions with different units of activity were used to stop bleeding in the rat-tail amputation model. Thrombin solutions can trigger fibrinogen to form fibrin and further form coagulation. Increasing the unit of activity will cause the thrombin solution to accelerate blood clotting (Fig. 5a). It is obvious that there is a striking correlation between thrombin amount and hemostatic time. However, when the thrombin solutions were sprayed onto the surface of CGS, the above-described dose relationship was different. Fig. 5b shows that when the amount of thrombin was increased from 5 U to 25 U, the hemostatic time of the obtained TCGS progressively shortened. In contrast, further increasing the amount of thrombin (to 50 U and 100 U) caused the hemostatic time of the TCGS to lengthens. These results indicated that the appropriate thrombin amount is a key factor for the hemostatic performance in the TCGS. Excessive thrombin shows no enhanced effect on clotting and may account for the attenuated absorbability of the TCGS.

On the other hand, although the amount of thrombin in the TCGS was 25 U, its hemostatic performance was close to that of 50 U thrombin solutions, showing the fact that the fast absorption capability of the TCGS also plays a pivotal part in its hemostasis. It needs a balance between thrombin stimulation and plasma absorption for the TCGS. Only by means of the synergy between fast absorption

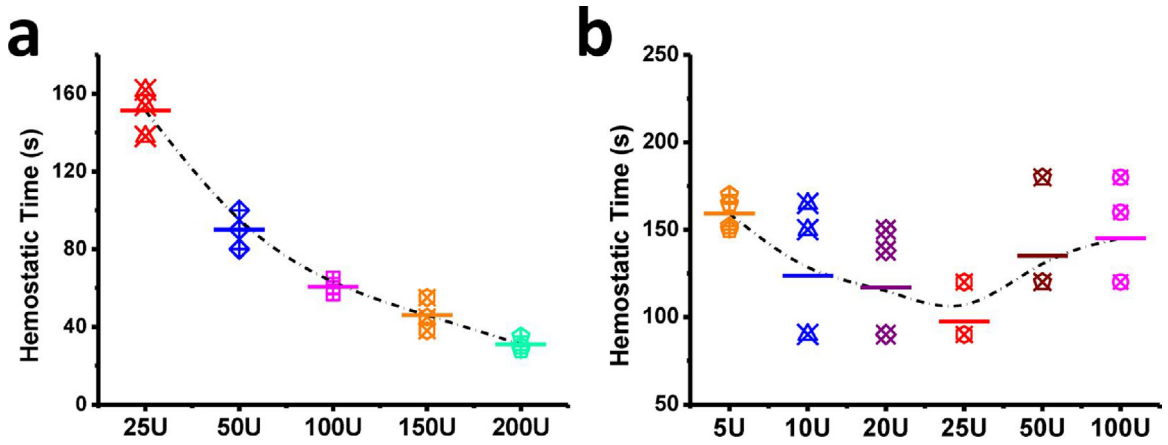

The hemostatic time of (a) the thrombin solutions (25, 50, 100, 150 and 200 U/mL) and (b) the TCGSs with different added amounts of thrombin (5, 10, 25, 50, 100 U). Data values correspond to the mean ± SD, n = 4.

and thrombin stimulation is the TCGS capable of ultrafast bleeding cessation.

With the aim of clarifying the influence of the thrombin amount on the absorbability, blood absorption rates of the TCGSs were tested using a high-speed camera. In Fig. 6, the $TCGS_{10}$ (10 U of added thrombin) completely absorbed a blood droplet within 40 ms, which is similar to that of CGS [14]. However, the absorption rate decreased to 200 ms when 25 U of thrombin was added (the typical TCGS). With the addition of more thrombin, 50 U and 100 U, the absorption rate decreased sharply to 360 ms and 720 ms, respectively. These results confirm that the absorbability of the TCGS is measurably affected by the addition amount of thrombin. In addition, this should be the reason why the $TCGS_{50}$ and $TCGS_{100}$ showed lower hemostatic efficiency than the typical TCGS.

3.6. Synergy mechanism

Scheme 1a represents the double mechanisms of the hemostatic performance of the TCGS. The hemostatic sponge CGS can rapidly absorb the plasma and aggregate hemocytes at the interface [14]. Meanwhile, the embedded thrombin acts as a coagulant to accelerate the formation of a blood scab. However, thrombin added to the CGS should be in the appropriate amounts (Scheme 1b). On one hand, thrombin addition should not block the pore structure of the TCGS so that the absorption capability of TCGS can be maximally maintained. On the other hand, thrombin on the surface of the TCGS should have sufficient enzyme activity to efficiently trigger the formation of fibrin. When the plasma is rapidly absorbed, the aggregated blood scab will be further reinforced by the newly formed fibrin (Scheme 1c). Thus, only by the synergy of these effects does the TCGS possesses excellent hemostatic performance. When less thrombin was used, although the absorption capability was maintained, the stimulation caused by thrombin was limited. The coagulation effect of the thrombin could not fully delivered. Conversely, excessive thrombin will block the pore structure of the TCGS. As a result, the hemocytes cannot be separated from the plasma, which slows the formation of the blood clot (Scheme 1b,c). That is, adding neither less nor an excessive amount of thrombin could improve the hemostatic performance of the TCGS. Therefore, both fast absorption and thrombin stimulation are important for its hemostatic performance. The physical absorbability and the biological stimulation should be balanced in this system, i.e., the synergistic effect is crucial for this composite, where both the CGS and thrombin maximize their contribution to hemostasis.

In addition to evoking the synergy effect, TCGS also presents composite advantages. First, the added amount of thrombin is 25 U, which is far lower than the clinically recommended concentration, 1000 U [50]. This dosage, combined with the composite manner of enrichment on the top layer of the CGS, not only effectively reduces the cost of thrombin but also makes the best use of both the thrombin and CGS. Second, the TCGS can be peeled off from the wound after bleeding has stopped. The immobilized thrombin within the TCGS is difficult to be flushed away or diffused into blood vessels, thus ensuring its biosafety because overuse of thrombin may cause serious complications, such as thromboembolism, heart failure, disseminated intravascular coagulation, and even life-threatening hemorrhage [23,33,51]. Although other carriers, such as polymers, gelatin, and silk fibroin are usually used to anchor thrombin in order to manage its release and reinforced its stability [26–28], most of those composites focus on in vivo applications and the enriched thrombin in the wound still poses the risk of causing thrombus. Hence, thrombin effectiveness is advanced in the TCGS for traumatic hemostasis.

4. Conclusions

In summary, we developed a facile spray method for preparing a TCGS composite. The spraying process is a soft and efficient method to introduce thrombin into the CGS. It does not produce any harsh physical or chemical changes, thus effectively protecting the biological activity of the thrombin. The CGS is also proved to be an ideal thrombin carrier because its high specific area and porous structure ensured that the immobilized thrombin fully contacted with blood cells to perform high-efficient catalytic capacity. In the synergy of fast plasma absorption and optimal thrombin stimulation, the TCGS exhibits outstanding hemostatic performance. It very rapidly stops bleeding, within 100 s. In addition, this TCGS composite has a high level of biosafety and stability. With a lower dosage of thrombin but superior efficiency, the TCGS composite allows for the maximal contribution of each constituent for bleeding control. Even stored for 6 months at the ambient temperature, the TCGS could still maintain excellent hemostatic performance. This property prolongs the shelf life and is conducive to the practical applications of the TCGS. Compared with traditional thrombin-based hemostats, the TCGS demonstrated many good features besides improved efficacy, such as facile preparation and utilization, low cost, portability and a long shelf life. Moreover, it is apparent that the synergic action between plasma absorption and thrombin stimulation is critical for high-performance of hemostasis. We confirmed that this graphene sponge is an excellent platform to carry multiple hemostats, and we have developed a more attractive TCGS-type hemostatic composites with superb performance and potentially new understandings.

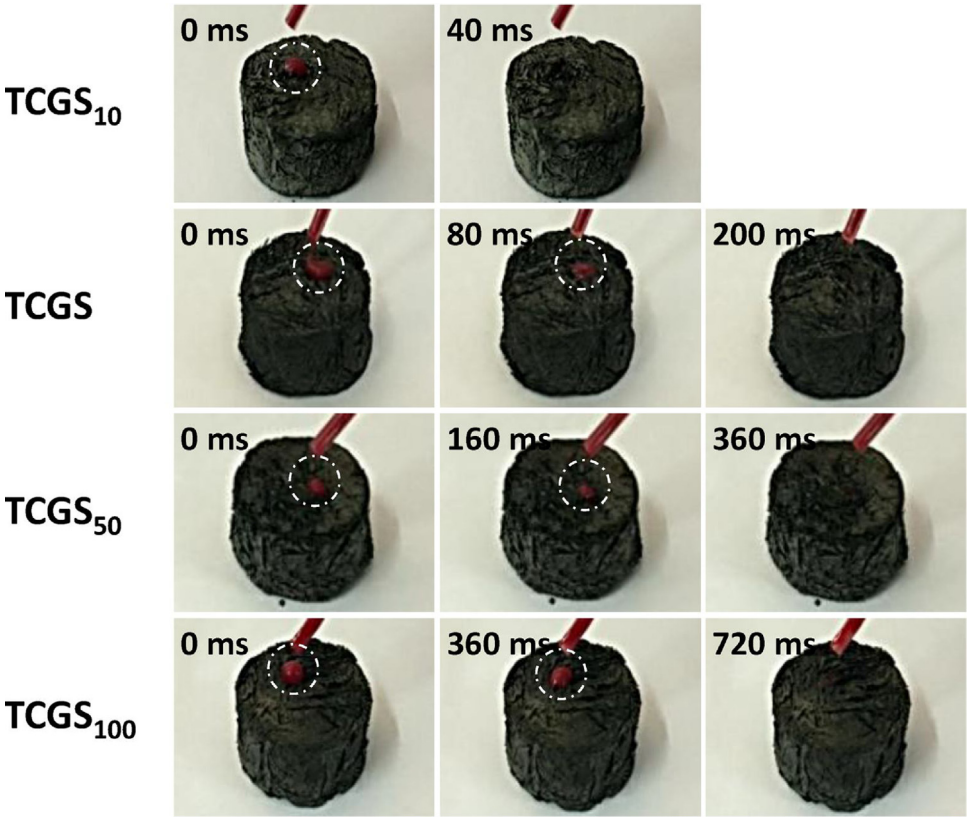

A high-speed camera (40 ms per frame) recorded the blood absorption rate of the TCGSs. $TCGS_{25}$ represents the typical TCGS.

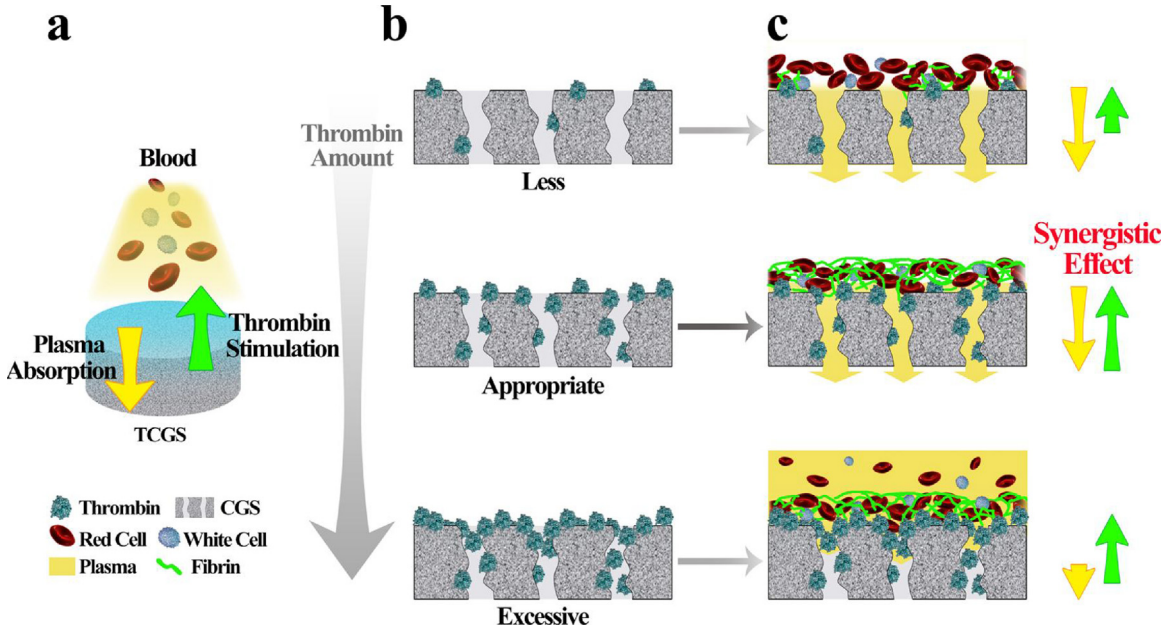

Schematic representation of the TCGS constructions and the synergy effect for hemostasis. (a) The hemostatic mechanisms of TCGS through the synergy effect of rapid plasma adsorption and thrombin stimulation. (b) Effects of the addition amount of thrombin on the porous structure of TCGS. (c) The appropriate addition amount of thrombin can effectively trigger blood clotting and, at the same time, maintain fast plasma absorbability. In the synergy of these two effects, TCGS achieved an outstanding hemostatic performance. While adding less or an excessive amount of thrombin showed less of a synergy effect for hemostasis. The length of the yellow or green arrows represents the strength of the related performance. (For interpretation of the references to colour in this figure legend, the reader is referred to the web version of this article.)

Acknowledgements

The authors thank the National Natural Science Foundation of China (21574008), and the Fundamental Research Funds for Central Universities (PYBZ1709, XK1701, BHYC1705B) for their funding support. Dr. Xing Wang also gratefully acknowledges China Scholarship Council for their financial support on a Visiting Scholar

Program (No. 201706885008) and the kind cooperation with Prof. James Liang in Stevens Institute of Technology, Hoboken, NJ 07030, U.S.A.

References

[1] C. Valdez, B. Sarani, H. Young, R. Amdur, J. Dunne, L.S. Chawla, J. Surg. Res. 200 (2016) 604–609.
[2] L.W. Chan, X. Wang, H. Wei, L.D. Pozzo, N.J. White, S.H. Pun, Sci. Transl. Med. 7 (2015) 277ra29.
[3] S. Saar, A. Lomp, J. Laos, V. Mihnovitš, R. Šalkauskas, T. Lustenberger, M. Väli, U. Lepner, P. Talving, World J. Surg. 41 (2017) 1–6.
[4] L.W. Chan, C.H. Kim, X. Wang, S.H. Pun, N.J. White, T.H. Kim, Acta Biomater. 31 (2016) 178–185.
[5] D. Chimene, D.L. Alge, A.K. Gaharwar, Adv. Mater. 27 (2015) 7261–7284.
[6] C. Chen, Y. Zhang, R. Fei, C. Cao, M. Wang, J. Wang, J. Bai, H. Cox, T. Waigh, J.R. Lu, H. Xu, ACS Appl. Mater. Interfaces 8 (2016) 17833–17841.
[7] Y. Bu, L. Zhang, J. Liu, L. Zhang, T. Li, H. Shen, X. Wang, F. Yang, P. Tang, D. Wu, ACS Appl. Mater. Interfaces 8 (2016) 12674–12683.
[8] C. Feng, J. Li, G. Wu, Y. Mu, M. Kong, C. Jiang, X. Cheng, Y. Liu, X. Chen, ACS Appl. Mater. Interfaces 8 (2016) 34234–34243.
[9] Z. Qian, H. Wang, X. Tuo, H. Guo, P. Xu, D. Liu, Y. Wei, H. Liu, X. Guo, J. Mater. Chem. B 5 (2017) 4845–4851.
[10] Q. Chen, Y. Liu, T. Wang, J. Wu, X. Zhai, Y. Li, W.W. Lu, H. Pan, X. Zhao, J. Mater. Chem. B 5 (2017) 3686–3696.
[11] H.E. Achneck, B. Sileshi, R.M. Jamiolkowski, D.M. Albala, M.L. Shapiro, J.H. Lawson, Ann. Surg. 251 (2010) 217–228.
[12] A.K. Gaharwar, R.K. Avery, A. Assmann, A. Paul, G.H. McKinley, A. Khademhosseini, B.D. Olsen, ACS Nano 8 (2014) 9833–9842.
[13] S.Y. Ong, J. Wu, S.M. Moochhala, M.H. Tan, J. Lu, Biomaterials 29 (2008) 4323–4332.
[14] K. Quan, G. Li, D. Luan, Q. Yuan, L. Tao, X. Wang, Colloids Surf. B 132 (2015) 27–33.
[15] K. Quan, G. Li, L. Tao, Q. Xie, Q. Yuan, X. Wang, ACS Appl. Mater. Interfaces 8 (2016) 7666–7673.
[16] G. Li, K. Quan, Y. Liang, T. Li, Q. Yuan, L. Tao, Q. Xie, X. Wang, ACS Appl. Mater. Interfaces 8 (2016) 35071–35080.
[17] A. Shukla, J.C. Fang, S. Puranam, F.R. Jensen, P.T. Hammond, Adv. Mater. 24 (2012) 492–496.
[18] Z. Wei, B.D. Elder, R. Goodwin, T.F. Witham, J. Clin. Neurosci. 22 (2015) 1502–1505.
[19] M. Emilia, S. Luca, B. Francesca, B. Luca, S. Paolo, F. Giuseppe, B. Gianbattista, M. Carmela, M. Luigi, L. Mauro, Transfus. Apher. Sci. 45 (2011) 305–311.
[20] J.T.B. Crawley, S. Zanardelli, C.K.N.K. Chion, D.A. Lane, J. Thromb. Hemostasis 5 (2007) 95–101.
[21] M.B. Ponczek, M.Z. Bijak, P.Z. Nowak, J. Mol. Evol. 74 (2012) 319–331.
[22] P.A. Nelson, J.N. Powers, T.D. Estridge, E.A. Elder, A.D. Alea, P.K. Sidhu, L.C. Sehl, F.A. DeLustro, J. Biomed. Mater. Res. Part A 58 (2001) 710–719.
[23] C.M. Cheng, C. Meyer-Massetti, S.R. Kayser, Clin. Ther. 31 (2009) 32–41.
[24] V.G. Nielsen, S.R. Paidy, W. McLeod, A. Fox, V.N. Nfonsam, J. Thromb. Thrombolysis 43 (2017) 423–425.
[25] W.C. Chapman, N. Singla, Y. Genyk, J.W. McNeil, K.L. Renkens, T.C. Reynolds, A. Murphy, F.A. Weaver, J. Am. Coll. Surgeons 205 (2007) 256–265.
[26] B. Zhuang, Z. Li, J. Pang, W. Li, P. Huang, J. Wang, Y. Zhou, Q. Lin, Q. Zhou, X. Ye, H. Ye, Y. Liu, L. Zhang, R. Chen, Int. J. Nanomed. 10 (2015) 939–947.
[27] J. Rong, M. Liang, F. Xuan, J. Sun, L. Zhao, H. Zhen, X. Tian, D. Liu, Q. Zhang, C. Peng, T. Yao, F. Li, X. Wang, Y. Han, W. Yu, Int. J. Biol. Macromol. 75 (2015) 479–488.
[28] R. Smeets, F. Gerhards, J. Stein, R.M. Pereira Paz, S. Vogt, C. Pautke, J. Weitz, A. Kolk, J. Biomed. Mater. Res. Part A 96 (2011) 177–185.
[29] G. Docimo, S. Tolone, R. Ruggiero, G. del Genio, L. Brusciano, A. Pezzolla, G. Jannelli, A. Bosco, D. Parmeggiani, C. Cosenza, P. Limongelli, L. Docimo, Int. J. Surg. 12 (2014) S209–S212.
[30] R. Watrowski, C. Jaeger, J. Forster, In Vivo 31 (2017) 251–258.
[31] I.S. Gill, A.P. Ramani, M. Spaliviero, M. Xu, A. Finelli, J.H. Kaouk, M.M. Desai, Urology 65 (2005) 463–466.
[32] D. Dimitroulis, E. Antoniou, N.P. Karidis, K. Kontzoglou, G. Kouraklis, Int. J. Surg. Case Rep. 3 (2012) 471–473.
[33] M.B. Ferschl, M.D. Rollins, Anesth. Analg. 108 (2009) 434–436.
[34] K. Steinestel, A. Geiger, R. Naraghi, U. Kunz, B. Danz, K. Kraft, G. Freude, Hum. Pathol. 44 (2013) 294–298.
[35] R. Gazzeri, M. Galarza, C. Conti, C. De Bonis, Neurosurg. Rev. (2017) 1–8.
[36] J. Liu, S. Fu, B. Yuan, Y. Li, Z. Deng, J. Am. Chem. Soc. 132 (2010) 7279–7281.
[37] X. Zhang, J. Yin, C. Peng, W. Hu, Z. Zhu, W. Li, C. Fan, Q. Huang, Carbon 49 (2011) 986–995.
[38] M.M. Bradford, Anal. Biochem. 72 (1976) 248–254.
[39] R. Gu, W. Sun, H. Zhou, Z. Wu, Z. Meng, X. Zhu, Q. Tang, J. Dong, G. Dou, Biomaterials 31 (2010) 1270–1277.
[40] C. Dai, Y. Yuan, C. Liu, J. Wei, H. Hong, X. Li, X. Pan, Biomaterials 30 (2009) 5364–5375.
[41] M.F. Shih, M.D. Shau, M.Y. Chang, S.K. Chiou, J.K. Chang, J.Y. Cherng, Int. J. Pharm. 327 (2006) 117–125.
[42] S.Y. Ong, J. Wu, S.M. Moochhala, M.H. Tan, J. Lu, Biomaterials 29 (2008) 4323–4332.
[43] P.T. Sudheesh Kumar, V.K. Lakshmanan, T.V. Anilkumar, C. Ramya, P. Reshmi, A.G. Unnikrishnan, S.V. Nair, R. Jayakumar, ACS Appl. Mater. Interfaces 4 (2012) 2618–2629.
[44] K.A. Tanaka, N.S. Key, J.H. Levy, Anesth. Analg. 108 (2009) 1433–1446.
[45] F.A. Ofosu, S. Crean, M.W. Reynolds, Clin. Ther. 31 (2009) 679–691.
[46] M.R. de Queiroz, B.B. de Sousa, D.F. da Cunha Pereira, C.C.N. Mamede, M.S. Matias, N.C.G. de Morais, J. de Oliveira Costa, F. de Oliveira, Toxicon 133 (2017) 33–47.
[47] M. Hoffman, D.M. Monroe, Hematol. Oncol. Clin. N. Am. 21 (2007) 1–11.
[48] N.L. Esmon, R.C. Carroll, C.T. Esmon, J. Biol. Chem. 258 (1983) 12238–12242.
[49] M. Handel, J. Winkler, R. Hörnlein, H. Northoff, P. Heeg, S. Sell, Arch. Orthop. Trauma Surg. 122 (2002) 269–273.
[50] D.C. Morse, E. Silva, J. Bartrom, K. Young, E.J. Bass, D. Potter, T. Bieber, J. Thromb. Thrombolysis 42 (2016) 352–359.
[51] M.C. Oz, J.F. Rondinone, N.S. Shargill, J. Card. Surg. 18 (2003) 486–493.